

© 2020. W. Piątkiewicz, P. Narloch, B. Pietruszka.

This is an open-access article distributed under the terms of the Creative Commons Attribution-NonCommercial-NoDerivatives License (CC BY-NC-ND 4.0, <https://creativecommons.org/licenses/by-nc-nd/4.0/>), which permits use, distribution, and reproduction in any medium, provided that the Article is properly cited, the use is non-commercial, and no modifications or adaptations are made.



INFLUENCE OF HEMP-LIME COMPOSITE COMPOSITION ON ITS MECHANICAL AND PHYSICAL PROPERTIES

W. Piątkiewicz¹, P. Narloch², B. Pietruszka³

The following work analyzes the effect of the composition of a hemp-lime composite on key mechanical and physical properties. The article contains results from testing the compressive strength, vapor permeability, and thermal conductivity of the composite, depending on the composition of the mix. The mixes differed from each other in binder composition and in the proportion of binder to hemp shives. The obtained results were compared with the results from other scientific literature. Based on this, conclusions were drawn that the binder composition is of secondary importance for the analyzed physical and mechanical properties of the hemp-lime composite. The main property that determines the values of the thermal conductivity coefficient as well as the compression strength is the density of the material, which depends on the proportion of binder to aggregate and the level of compaction of the mix. The value of the diffusion resistance coefficient of the analyzed material was very low regardless of the composition of the composite.

Key words:

Keywords: hemp-lime composite, hempcrete, compressive strength, thermal conductivity, vapour diffusion resistance factor, sustainable building material

¹ MSc., Eng., Warsaw University of Technology, Faculty of Civil Engineering, Al. Armii Ludowej 16, 00-637 Warsaw, Poland, e-mail: wojtek.piat@gmail.com

² PhD., Eng., Warsaw University of Technology, Faculty of Civil Engineering, Al. Armii Ludowej 16, 00-637 Warsaw, Poland, e-mail: p.narloch@il.pw.edu.pl

³ PhD., Building Research Institute, Department of Thermal Physics, Acoustics and Environment, Ksawerów 21, 02-656 Warszawa, Poland, e-mail: b.pietruszka@itb.pl

1. INTRODUCTION

1.1. HEMP-LIME COMPOSITE AS A SUSTAINABLE BUILDING MATERIAL

According to the United Nations Environment Programme, the construction industry is responsible for 36% of global energy consumption and almost 40% of total carbon dioxide emissions [1]. Embodied carbon dioxide emissions account for as much as 15% of the total calculated emissions for a building's entire lifetime [1]. Embodied emissions are a measure of the cumulative greenhouse gas emissions caused by the production, transport, and use of a specific product. As the energy efficiency of buildings increases, the percentage of embodied emissions out of the total greenhouse gas emissions released during a building's life cycle will increase. For a 100-year lifespan, embodied energy increases from 8% to 60% of the total energy consumption for buildings with a heating demand of 200 kWh/m²/year and 15 kWh/m²/year, respectively [2]. Accordingly, material and technological solutions with the lowest energy demand and the lowest possible carbon footprint should be sought.

A hemp-lime composite is a material that has a negative carbon footprint [3]. Due to the fact that this material is primarily composed of plants that absorb carbon dioxide during their lifetime, and the main binder component is hydrated lime, which needs carbon dioxide to be able to react, a lime-hemp composite is a great opportunity to reducing greenhouse gas emissions in construction [3], [4]. Hemp-lime composite is mainly used as a thermal insulating material that fills the skeletal structure of a building [3]. A commonly used method is to place fresh composite mix in a formwork between a wooden structure [5]. Hemp-lime composite is produced on the construction site [5].

An analysis was made in [3], in which five different external partitions were compared [Fig. 1]. Each had the same heat transfer coefficient value $U=0.125$ W/m²k, each was load bearing, and each had a lifespan of 60 years considering appropriate maintenance for each material. A wall of pressed straw blocks within a timber structure (Fig. 1, STRAW), a wall made of hemp-lime composite with a timber structure (Fig. 1, HEMPCRETE), a wall with a timber frame with glass wool (Fig. 1, TIMBER), a wall of ceramic blocks with EPS insulation (Fig. 1, BRICK), and a wall of reinforced concrete with EPS insulation (Fig. 1, CONCRETE) were compared. The authors used the Dynamic Life Cycle Assessment method, which takes into account, inter alia, carbon dioxide storage and the delay of its emission by plants [3]. The method also considers carbon dioxide absorption and greenhouse gas emissions distributed over time [3]. The authors analyzed various options for recycling and

reutilization of materials, as well as the time needed to renew resources. In Fig. 1 is shown a variant that assumes all non-biogenic materials are landfilled, while bio-based materials are temporarily transferred to a sanitary landfill [3]. The hemp-lime wall consisted partly of prefabricated blocks 30 cm thick joined with lime mortar and a 20 cm thick composite with a ratio of shive to binder 1:1 sprayed on. The binder was a mix of hydrated dolomite lime (80%) and cement (20%). The analysis showed that fast-growing plant materials such as straw or hemp significantly reduce a building's carbon footprint. It is worth noting that the timber frame wall with glass wool (Fig. 1, TIMBER), did not turn out to be much better than the wall made of ceramic blocks (Fig. 1., BRICK) due to the long time needed for forests to regrow and renew biomass, of which the partition was largely composed of [3].

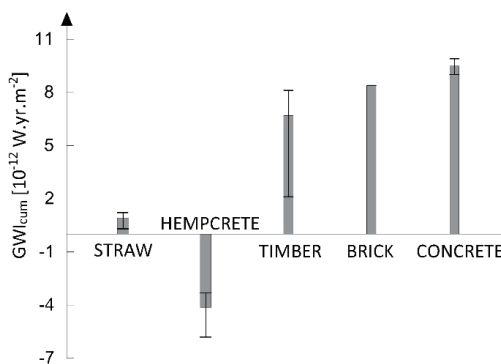


Fig. 1. Comparison of the cumulated Global Warming Impact (GWI_{cum}) for a 100 year period for partitions composed of various materials. The error bars represent the maximum and minimum deviations discussed in [3].

1.2. HEMP-LIME COMPOSITE COMPONENTS

The wooden part of a hemp plant is known as hemp shive. It accounts for 70% of the stem volume and is obtained in the process of decortication [6]. The structure of hemp shive is very porous with as much as 43% of its volume composed of air (total porosity of 57%) [6]. A network of closed pores with a size of 5 to 50 μm makes it a good heat-insulating material [6].

The main component of the binder is hydrated lime, accounting for 70-80% of the binder [6]–[15]. Other components include hydraulic lime, Portland cement and pozzolanic additives such as silica dust, fly ash or metakaolin [6]–[15]. These additives increase the compressive strength of the composite [12], [16].

Metakaolin is a pozzolana with a high degree of reactivity, which is formed by burning ground kaolin at a temperature of 650-800 °C [17]. A major advantage of this additive is an improvement in the durability of the material [2], [18], [19]. The metakaolin causes a reduction in the size of pores of the paste and the formation of denser and more stable hydrates. Hemp-lime composites where part of the binder is replaced with metakaolin are more resistant to sulphates, chlorides, freezing and thawing cycles, and alkaline reactions [2].

The main advantage of using metakaolin is its low environmental impact compared to other binder components. The energy consumption of the production process lower than for the production of Portland cement, hydrated lime, and hydraulic lime [2], [20]. Metakaolin may also be a by-product of the production process of porous glass granulate [7].

1.3. PROPERTIES OF HEMP-LIME COMPOSITE

1.3.1. MECHANICAL PROPERTIES

Hemp shives are flexible and porous, causing them to yield without breaking or tearing under applied loads. The material also exhibits high deformability under pressure [16]. Hemp-lime composite is not a structural material; depending on the density, the material can achieve a compressive strength from 0.05 MPa to 3.5 MPa [21]. Most often the value falls within the range of 0.18 to 0.85 MPa [22].

Based on the mode of failure, the compressive strength is determined in two ways. The first is the continuous loading of the sample until a change in the dependence of stress on deformation occurs, which appears at about 10% deformation [9]. In some tests, the maximum compressive strength is assumed to be at 20% deformation of the lime-hemp composite samples [12]. The ratio of binder to shives is crucial for keeping the composite together under loading [6], [7], [11], [14], [16]. As the material's density increases, so does its compressive strength [6], [7], [16], [8]–[15].

1.3.2. PHYSICAL PROPERTIES

The thermal conductivity coefficient of dry hemp-lime composite ranges from 0.06 (for a density of 250 kg/m³) to 0.138 W/mK (for a density of 627 kg/m³) [21]. The density of the composite has a major influence on its thermal conductivity [6]. According to [5], the value of the thermal conductivity coefficient of hemp-lime composite is also dependent on the type of binder. A higher content of hydraulic components increases the value of the thermal conductivity coefficient [5], [23].

On the other hand, according to [7], the binder composition has little effect on the thermal conductivity of hemp-lime composite.

The diffusion resistance coefficient for hemp-lime composite, depending on the density of the mix and the composition of the binder, ranges from 3.59 to 7.68 [21]. The main factor that affects the vapor permeability of a hemp-lime composite is the porous structure of hemp shive. Binders that have a smaller content of hydraulic components have a lower diffusion resistance coefficient [9]. Macropores between hemp particles have a greater influence on vapor permeability than micropores in the binder structure [9].

2. MATERIALS AND METHODS

2.1. MATERIALS

The study used a French strain of hemp “Futura 75”. The hemp shive, which was partially separated from fiber, had a length of 5-25 mm. Binder components are shown in Table 1. The main ingredient of the binder was hydrated lime CL 90s according to EN 459-1:2003. In addition, hydraulic trass lime NHL 3.5 according to EN 459-1:2003 was also used. Metakaolin was used as a pozzolanic additive. To obtain different densities of composite, two proportions of aggregate to binder were used (Table 2). The amount of water used in the mixes as shown based on [6], [9], [14].

Table 1. Binder compositions used in referenced studies.

Binder Composition	Hydrated lime CL 90S	Hydrated lime NHL 3.5	Metakaolin „Astra MK 40”
I, II	80%	-	20%
III, IV	70%	15%	15%

Table 2. Proportions of ingredients for each series used in this study.

Proportion of ingredients in each series	Binder	Hemp Shive	Water
I	1.5	1	2.5
II	2	1	3.3
III	1.5	1	2.4
IV	2	1	2.8

The dry binder components were mixed first. Then $\frac{3}{4}$ by weight of water was added and mixed until a homogeneous suspension was obtained. Then hemp shives and the remaining water were added while stirring. All components were then combined in a mixer for 5-8 minutes until a homogeneous consistency was obtained. Before being placement into the mold, the mix was weighed in order to obtain the same density for all samples in a given series. The sample molds had been previously treated with an anti-adhesive agent. The lime-hemp composite was placed in layers of 5 cm and vigorously compacted with a 5x5 cm beater with a weight of 0.5 kg. Compaction of the mix was done to evenly distribute the material and eliminate irregular air voids. Cubic samples with dimensions of 10x10x10 cm, cylindrical samples with a diameter of 12.8 cm and height of 6 cm, as well as plate samples with dimensions of 30x30x6 cm were made. All samples were equally compacted. Samples were cured for 28 days at a temperature of $20\pm 2^{\circ}\text{C}$ with a relative humidity of $65\pm 5\%$. After 24 hours the samples were demolded. Sample density was measured at ambient conditions.

2.2. METHODS

2.2.1. THERMAL CONDUCTIVITY TEST

The test was conducted in accordance with standard EN 12667 [24]. Immediately before testing, the samples were stored in a space with a temperature of $23\pm 5^{\circ}\text{C}$ and relative humidity of $50\pm 5\%$ until the mass stabilized. Thermal conductivity measurements were done in a stabilized state using the “hot plate” method in a FOX 314 plate apparatus (Fig. 2.). The temperature difference between the upper and lower plates was 20 K, with the sample temperature being 10°C . Heat flowed in a direction perpendicular to the molding direction, from the bottom to the top. The samples each had a dimension of 30x30 cm with a thickness of 6 cm. Tests were carried out on 10 samples of each series.



Fig. 2. Thermal conductivity test.

2.2.2. VAPOR PERMEABILITY TEST

The test was conducted in accordance with standard EN 12086 [25]. Immediately before testing, the samples were stored in a space with a temperature of $23\pm 5^{\circ}\text{C}$ and relative humidity of $50\pm 5\%$ until the mass stabilized with a 5% tolerance. Next, cylindrical samples with a diameter of 12.8 cm and a height of 6 cm were placed in metal dishes on the bottom of which was a drying agent (CaCl_2). Changes in mass were measured for a 24-hour period. The study was terminated when five consecutive changes in the mass per unit time are constant and housed within a tolerance of $\pm 5\%$ of the average for each sample tested. The tolerance for each test was 5% relative to the average of each sample. Tests were carried out on 10 samples of each series.

2.2.3. COMPRESSIVE STRENGTH TEST

The compressive strength test was carried out in a compression testing press. The machine allowed for a gradual application of loading, which was especially advantageous. A constant load increase of 1.5 kN/min was assumed. The test samples were cubes with sides of 10 cm. The samples were compressed in the direction of the layering of the mix, which is how hemp concrete works when made using the formwork method. Tests were carried out on 10 samples of each series.

3. RESULTS

3.1. COMPRESSIVE STRENGTH

Median values for the compressive strength results of all series are shown in Fig. 3. The compressive strength of Series II relative to Series I at 20% deformation increased by 78.12%. The increase in compressive strength between Series III and IV at 20% deformation was 50.86%.

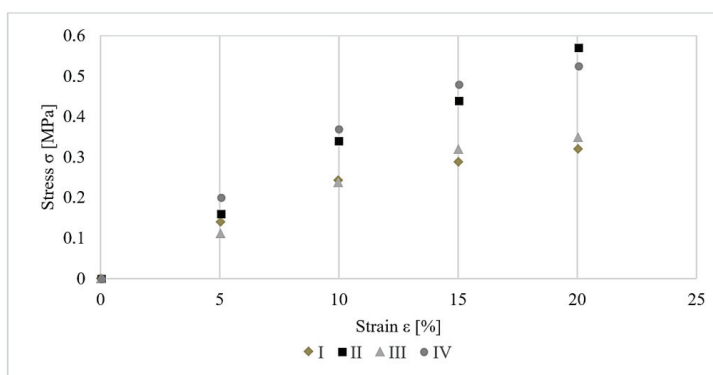


Fig. 3. Compressive strength (median) for each sample series.

3.2. THERMAL CONDUCTIVITY

The increase in the proportion of binder to aggregate caused a 22.71% increase in density between series I and series II, and 21.6% when comparing series III and series IV. Thermal conductivity coefficient results are shown in Fig 4. Thermal conductivity increased along with the density of the material. The type of binder had a secondary influence on sample density. Thermal conductivity increased along with the binder content in the composite mix. The average thermal conductivity coefficient of composite samples of series II was 3.47% higher than that of series I, while the average of series IV was 9.37% higher than that of series III. Series I had a worse thermal conductivity coefficient compared to series III by 5.92%. The smallest difference in thermal conductivity occurred between series II and IV, with a difference of 0.56%. The ratio of shives to binder had a significant impact on thermal conductivity.

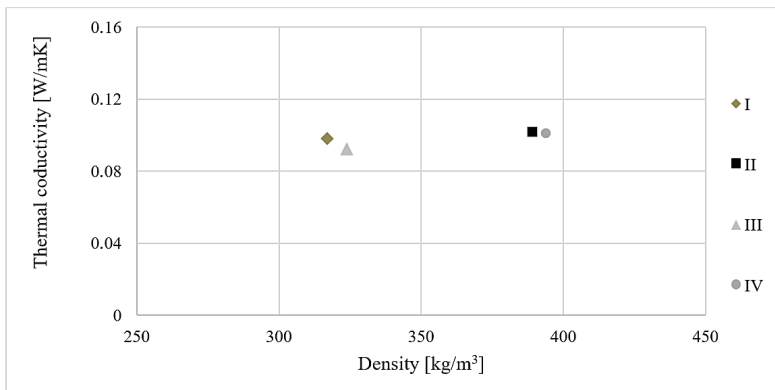


Fig. 4. Average thermal conductivity coefficient for each sample series.

3.3. VAPOR PERMEABILITY

The diffusion resistance coefficient of tested samples ranged from 4.2 to 6.45 (Fig. 5). The smaller the density was, the higher the value of thermal conductivity became. There was no significant difference between series I and III or series II and IV. Series II had a poorer vapor permeability than Series I by 13.4%, however, series IV differed from series III by 6.25%.

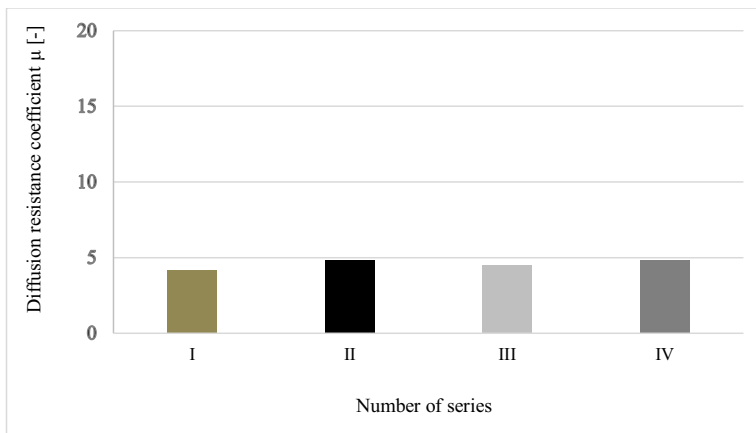


Fig. 5. Diffusion resistance coefficient for each series.

4. DISCUSSION

4.1. HEMP-LIME COMPOSITE THERMAL CONDUCTIVITY

Thermal conductivity values obtained by the authors or located in [6], [11], [15], [21], [26], [27] are shown in Fig. 6 and Table 3. All results were obtained through the same thermal conductivity testing method, in a plate apparatus. Test results are displayed with the various articles denoted by color, while compositions are marked by different shapes. An analysis of the results leads to the conclusion that the main factor affecting thermal conductivity is the density of the material. It was noted that thermal conductivity changes approximately linearly with increasing density, regardless of the composition of the mix. Changing the binder does not significantly change the density of the material. The material density is primarily determined by the ratio of binder to shives and the degree of compression. This implies that it is possible to design a material with thermal conductivity based on its density. A high ratio of shives to binder leads to the formation of a sizable amount of macropores in hemp-lime composites, in which the level of heat exchange is higher (Fig. 7). Therefore, although the density was lower, the thermal conductivity did not decrease significantly.

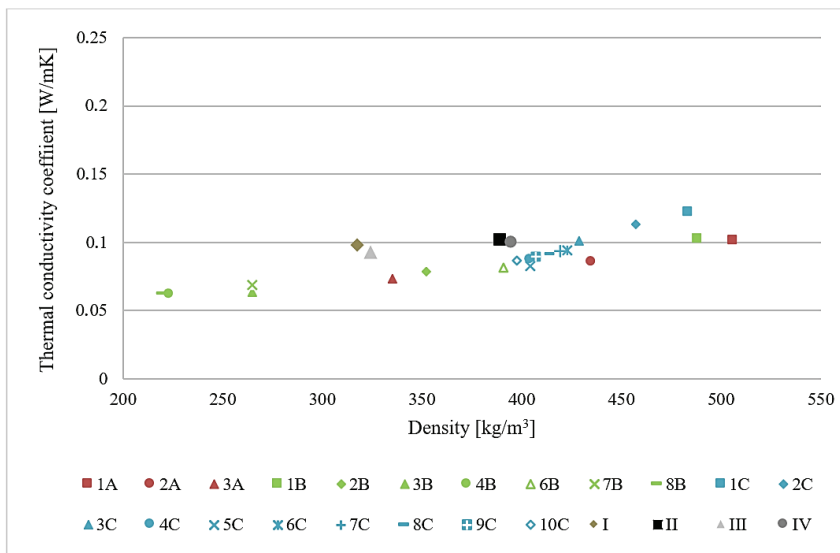


Fig. 6. Thermal conductivity coefficients of hemp-lime composite depending on the density of the material.

The author's results are named I, II, III and IV. Symbol descriptions are given in Table 3.



Fig. 7. The structure of hemp-lime composites with a hemp-lime ratio of 1:2 (right) and 1:1,5 (left).

Table 3. Detailed summary of hemp-lime composite mix components and their properties. Results obtained from this study have a gray background.

Source	Composite symbol	Density	Binder [%]									Proportions			Results					
			Hydrated lime	CEM II/B-V 32,5 R	Metakaolin	Fireclay mortar ZZSz 0-2	Loam	Gypsum	Hydraulic lime	Ground Granulated Blastfurnace Slag	Roman cement	Binder	Hemp shives	Water	Thermal conductivity coefficient [W/mK]	Compressive strength at 10% deformation [Mpa]	Compressive strength at 20% deformation [Mpa]	Diffusion resistance coefficient [-]		
[27]	1A	506	28	24	24	24							1.4	1	0.93	0.102	-	-	3.6	
	2A	435	27	24	24	25							1.37	1	0.97	0.085	-	-	3.8	
	3A	335	25	25	25	25							1.33	1	1	0.073	-	-	4	
[7]	1B	488	60	40									2.5	1	nd	0.103	0.435 ^a	-	-	
	2B	352											2	1	nd	0.079	0.111 ^a	-	-	
	3B	265											1	1	nd	0.064	0.071 ^a	-	-	
	4B	223											0.75	1	nd	0.062	0.062 ^a	-	-	
	5B	459	70	10									2.5	1	nd	0.101	0.570 ^a	-	-	
	6B	391											2	1	nd	0.081	0.204 ^a	-	-	
	7B	265											1	1	nd	0.069	0.105 ^a	-	-	
	8B	220											0.75	1	nd	0.063	0.071 ^a	-	-	
[6]	1C	483.5	70	15	15								2	1	2.8	0.122	-	0.32 ^b	-	
	2C	457.1											1.83	1	2.65	0.113	-	0.29 ^b	-	
	3C	428.6											1.67	1	2.5	0.101	-	0.26 ^b	5,94	
	4C	404.4											1.5	1	2.35	0.088	-	0.23 ^b	-	
	5C	404.6	70	23			7						1.43	1	2.86	0.082	-	0.51 ^b	5,52	
	6C	423.1	75	10										1.8	1	2.79	0.094	-	0.44 ^b	5,82
	7C	419.5												1.7	1	2.67	0.093	-	0.37 ^b	-
	8C	414.6												1.6	1	2.56	0.091	-	0.32 ^b	-
	9C	407.1												1.5	1	2.45	0.089	-	0.28 ^b	-
	10C	397.7												1.4	1	2.31	0.086	-	0.22 ^b	-
11C	394.4	1.3												1	2.2	0.084	-	0.18 ^b	-	
Authors	I	317	80	20									1.5	1	2.5	0.098	0.244	0.32	-	
	II	389											2	1	3.3	0.102	0.34	0.57	-	
	III	324	70	15									1.5	1	2.4	0.093	0.24	0.348	-	
	IV	394											2	1	2.8	0.101	0.37	0.525	-	
[10]	2F	350											100	2	1	2	0.104	-	0.18 ^c	-

Legend:

^a 28 days curing (20±2 °C and 40±10% RH), samples 100x100x(80-93)mm, 10% relative deformations

^b 28 days curing (20±2 °C and 55±5% RH), samples 150x150x150mm, 20% relative deformations

^c 90 days curing (20 °C and 65% RH), cylindrical samples with diameter 100mm and height 200mm, 20% relative deformations

^d 28 days curing, samples 50x50x50mm, 20% relative deformations

^e 365 days curing (16±3 °C and 55±10% RH), samples 100x100x100mm, 10% relative deformations

^f 28 days-6months curing (20 °C and 50% RH), cylindrical samples diameter 160mm and height 320mm, 10% relative deformations

nd – no data

Table 4. (continued)

Source	Composite symbol	Density	Binder [%]									Proportions			Results					
			Hydrated lime	CEM II/B-V 32,5 R	Metakaolin	Fireclay mortar ZZSz 0-2	Loam	Gypsum	Hydraulic lime	Ground Granulated Blastfurnace Slag	Roman cement	Binder	Hemp shives	Water	Thermal conductivity coefficient [W/mK]	Compressive strength at 10% deformation [Mpa]	Compressive strength at 20% deformation [Mpa]	Diffusion resistance coefficient [-]		
[12]	1G	515	100										2	1	3	-	0.69 ^d	-		
	2G	510	80	20									2	1	3	-	0.73 ^d	-		
	3G	454								100			2	1	3	-	0.48 ^d	-		
	4G	435			20						80		2	1	3	-	0.35 ^d	-		
[9], [23]	1H	627	70	10				20					2	1	3.1	0,138	0.37 ^e	-	5.51	
	3H	564	70						30				2	1	3.1	0,126	0.41 ^e	-	5.56	
	4H	569											2	1	3.1	0,129	0.39 ^e	-	5.71	
	5H	508	80										2	1	3.3	0,117	0.34 ^e	-	5.42	
	6H	531		20									2	1	3.1	0,123	0.32 ^e	-	5.71	
[14]	1I	460											2.43	1	3.56	-	0.15 ^f	-	-	
	2I	480							100				2.45	1	3.04	-	0.27 ^f	-	-	
	3I	480											2.45	1	2.84	-	0.22 ^f	-	-	
	4I	390											1.99	1	3.18	-	0.31 ^f	-	-	
	5I	500											2.58	1	3.56	-	0.64 ^f	-	-	
	6I	460											2.43	1	3.56	-	0.44 ^f	-	-	
	7I	390	75	10					15					2.04	1	3.02	-	0.4 ^f	-	-
	8I	250									0.98	1	2	-	0.2 ^f	-	-			
	9I	400									1.99	1	3.18	-	0.34 ^f	-	-			
	10I	430									1.99	1	3.18	-	0.22 ^f	-	-			

Legend:

^a 28 days (20+2 deg C i 40+10% RH), samples 100x100x(80-93)mm, to 10% relative deformations

^b 28 days (20+2 deg C i 55+5% RH), samples 150x150x150mm, deformation 20%

^c 90 days (20 deg C i 65% RH), cylindrical samples with diameter 100mm and height 200mm, at 20% deformation

^d 28 days, samples 50x50x50mm, 20% deformation

^e 365 days (16±3 deg C and rel. humidity 55±10%), samples 100x100x100mm, „10% deformation”

^f 28 days-6months (20 degC i 50% RH), cylindrical samples diameter 160mm and height 320mm, at 10% deformation

nd – no data

4.2. HEMP-LIME COMPOSITE COMPRESSIVE STRENGTH

As mentioned earlier, the compressive strength of the hemp-lime composite is determined for different levels of deformation (Table 3). A comparison of results, however, is difficult due to the authors' use of separate articles containing samples of different shapes, humidity and curing times, and different methods for determining compressive strength. The highest compressive strength was achieved by the "2G" series [12], whose value was 0.73 MPa. Linseed oil was used in this study, which reduced aggregate water content and thus increased compressive strength. As can be seen, despite many variables, the compressive strength of the hemp lime composite is low, ranging from 0.062 to 0.73 MPa.

The results of compressive strength at 10% deformation, conducted on 100x100x100 mm cubic samples, are compared with each other in Fig. 8. The results obtained by the authors do not differ significantly from the results from [7], and are less than 0.6 MPa. This means that hemp-lime composite should not be used structurally. Analysis of the graph in Fig. 8 suggests that the compressive strength depends primarily on the density of the material, which in turn depends on the ratio of shives to binder and the method of compacting the mix. The level of compression in the analyzed results was the same. Binder composition has a secondary effect on the density of the material.

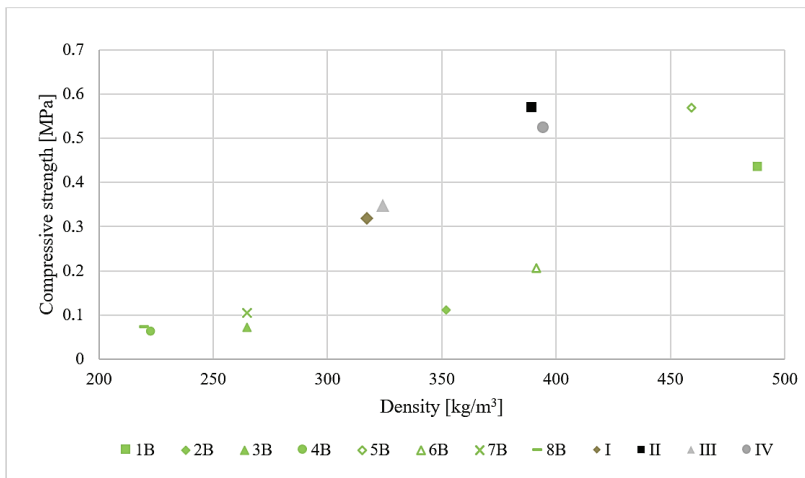


Fig. 8. Summary of compressive strength results as determined at 10% deformation. Symbol descriptions are given in Table 3.

4.3. HEMP-LIME COMPOSITE VAPOR PERMEABILITY

The vapor permeability of hemp-lime composite is described in [6], [23], [27]. The results obtained by the authors are very similar (Table 3, Fig. 5). It can be seen in Fig. 9 that the vapor permeability of hemp lime composite is slightly affected by the density and composition of the binder. The diffusion resistance coefficient of hemp-lime composite is small, ranging from about 4-6. This is valuable information that allows you to design the flow of vapor through partitions containing a layer of hemp-lime composite thermal insulation.

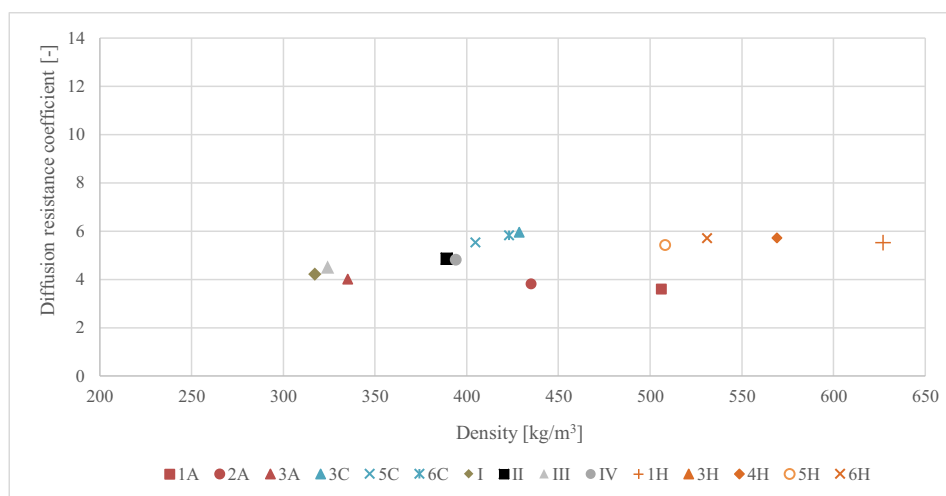


Fig. 9. Comparison of diffusion resistance coefficient results. Symbol description are given in Table 3.

5. CONCLUSIONS

Throughout the course of this study, it has been shown that density has a significant impact on the properties of hemp-lime composite. Also demonstrated is that density is dependent on the ratio of binder to aggregate. The type of binder used has a minor influence on the material's properties. For this reason, it is recommended to use the most ecological binders, such as metakaolin, so that the environmental impact of the material is minimized.

Analysis of the results concludes that the material should be expected to have a density of about 380 kg/m³. This density is obtained for a binder to shive ratio of 2. At higher shive contents, a sizable

amount of macropores is created, which reduces the thermal conductivity, while also decreasing the compressive strength.

The compressive strength of lime-hemp composite after 28 days of curing does not depend on the composition of the binder used in the mix. This property is primarily associated with the ratio of binder to shive. For the composites tested, the compressive strength ranged from 0.32 to 0.57 MPa at 20% deformation. A material with such a compressive strength is not recommended to be used structurally. When designing a hemp-lime composite, the key task should be to achieve such a compressive strength as to allow it to perform a self-supporting function while having the lowest possible thermal conductivity coefficient.

The composition of the hemp-lime composite does not have a significant influence on diffusion resistance, which in this study resulted in a value of 4-5. High vapor permeability can be both an advantage and a disadvantage, due to the possibility of condensation in the outer partition, among other effects. Therefore, a low value of diffusion resistance should be considered when designing the building envelope of hemp-lime composite buildings.

A major advantage of hemp-lime composite is its negative carbon footprint. Directing attention to the environmental cost of the material when planning an investment appears to play a key role in the dissemination of hemp-lime composite.

REFERENCES

- [1] Global Alliance for Buildings and Construction, International Energy Agency, i The United Nations Environment Programme (2019), „2019 global status report for buildings and construction: Towards a zero-emission, efficient and resilient buildings and construction sector.”, 2019.
- [2] A. Sofiane i A. Laurent, *Bio-aggregate-based building materials : applications to hemp concretes*, 1. wyd. John Wiley & Sons, Incorporated, 2013.
- [3] F. Pittau, F. Krause, G. Lumia, i G. Habert, „Fast-growing bio-based materials as an opportunity for storing carbon in exterior walls”, *Build. Environ.*, t. 129, nr August 2017, ss. 117–129, 2018.
- [4] M. Sinka, A. Korjakins, i D. Bajare, „Enhancement of lime-hemp concrete properties using different manufacturing technologies”, nr June, 2015.
- [5] F. Collet i S. Pretot, „Thermal conductivity of hemp concretes : Variation with formulation , density and water content”, *Constr. Build. Mater.*, t. 65, ss. 612–619, 2014.
- [6] P. Brzyski, „Hemp-lime composite as wall material meeting the requirements for sustainable development in construction industry”, Lublin University of Technology, 2018.
- [7] M. Sinka, P. Van Den Heede, N. De Belie, D. Bajare, i G. Sahmenko, „Comparative life cycle assessment of magnesium binders as an alternative for hemp concrete”, *Resour. Conserv. Recycl.*, t. 133, nr February, ss. 288–299, 2018.
- [8] W. Stanwix i A. Sparrow, *The Hempcrete Book*. Cohabitat Foundation, 2016.
- [9] R. Walker, S. Pavia, i R. Mitchell, „Mechanical properties and durability of hemp-lime concretes”, *Constr. Build. Mater.*, t. 61, ss. 340–348, 2014.
- [10] G. Delannoy i in., „Influence of binder on the multiscale properties of hemp concretes”, *Eur. J. Environ. Civ. Eng.*, t. 8189, ss. 1–17, 2018.
- [11] S. Benfratello, C. Capitano, G. Peri, G. Rizzo, G. Scaccianoce, i G. Sorrentino, „Thermal and structural properties of a hemp – lime biocomposite”, *Constr. Build. Mater.*, t. 48, ss. 745–754, 2013.
- [12] J. Sheridan i in., „Effect of linseed oil and metakaolin on the mechanical, thermal and transport properties of

- hemp-lime concrete”, 2017.
- [13] S. Elfordy, F. Lucas, i F. Tancrét, „Mechanical and thermal properties of lime and hemp concrete (“ hempcrete”) manufactured by a projection process”, t. 22, ss. 2116–2123, 2008.
- [14] L. Arnaud i E. Gourlay, „Experimental study of parameters influencing mechanical properties of hemp concretes”, *Constr. Build. Mater.*, t. 28, nr 1, ss. 50–56, 2012.
- [15] J. Williams, M. Lawrence, i P. Walker, „The influence of the casting process on the internal structure and physical properties of hemp-lime”, *Mater. Struct.*, t. 50, nr 2, ss. 1–10, 2017.
- [16] K. Sandin, C. Nilsson, P. Brigitte, i D. Bruijn, „Mechanical properties of lime – hemp concrete containing shives and fibres”, t. 103, ss. 474–479, 2009.
- [17] P. L. Narloch, P. Woyciechowski, i P. Jęda, „The Influence of Loam Type and Cement Content on the Compressive Strength of Rammed Earth”, *Arch. Civ. Eng.*, t. 61, nr 1, ss. 73–88, 2015.
- [18] P. L. Narloch, P. Woyciechowski, E. Dmowska, i K. Halemba, „Durability Assessment of Monolithic Rammed Earth Walls”, *Arch. Civ. Eng.*, t. 61, nr 2, ss. 73–88, 2015.
- [19] P. Narloch i P. Woyciechowski, „Assessing Cement Stabilized Rammed Earth Durability in A Humid Continental Climate”, *Buildings*, t. 10 (26), ss. 1–20, 2020.
- [20] P. Narloch, P. Woyciechowski, J. Kotowski, I. Gawriuczenkow, i W. Emilia, „The Effect of Soil Mineral Composition on the Compressive Strength of Cement Stabilized Rammed Earth”, *Materials (Basel)*, t. 13 (324), ss. 1–21, 2020.
- [21] U. Dhakal, U. Berardi, M. Gorgolewski, i R. Richman, „Hygrothermal performance of hempcrete for Ontario (Canada) buildings”, *J. Clean. Prod.*, t. 142, ss. 3655–3664, 2017.
- [22] P. Brzyski i S. Fic, „Characteristics of lime-hemp composite and its use in construction industry”, *Bud. i Architekt.*, t. 14, nr 2, ss. 11–19, 2015.
- [23] R. Walker i S. Pavia, „Moisture transfer and thermal properties of hemp – lime concretes”, *Constr. Build. Mater.*, t. 64, ss. 270–276, 2014.
- [24] „EN 12667:2001 Thermal performance of building materials and products. Determination of thermal resistance by means of guarded hot plate and heat flow meter methods - products of high and medium thermal resistance”.
- [25] „EN 12086:2013 Thermal insulating products for building applications. Determination of water vapour transmission properties”.
- [26] M. Sinka, A. Pina, P. Ferrão, J. Fournier, B. Lacarrière, i O. Le Corre, „In-situ measurements of hemp-lime insulation materials for energy efficiency improvement”, *Energy Procedia*, t. 147, ss. 242–248, 2018.
- [27] E. Haustein, „Thermal insulation properties of the lime-cement composite with hemp shives”, *Ecol. Eng.*, t. 19, nr 4, ss. 72–78, 2018.

LIST OF FIGURES AND TABLES:

Fig. 1. Comparison of the cumulated Global Warming Impact (GWI_{cum}) for a 100 year period for partitions composed of various materials. [3]. The error bars represent the maximum and minimum deviations discussed in [3].

Rys. 1. Porównanie skumulowanego wpływu na globalne ocieplenie (GWI_{cum}) na okres 100 lat dla przegród wykonanych z różnych materiałów [3]. Paski dokładności wyników przedstawiają maksymalne i minimalne odchyłki dyskutowane w [3].

Fig. 2. Thermal conductivity test.

Rys. 2. Badanie współczynnika przewodności cieplnej.

Fig 3. Compressive strength (median) for each sample series.

Rys. 3. Wyniki wytrzymałości na ściskanie (mediany) dla poszczególnych serii próbek.

Fig. 4. Average thermal conductivity coefficient for each sample series.

Rys. 4. Średni współczynnik przewodzenia ciepła poszczególnych serii próbek.

Fig 5. Diffusion resistance coefficient for each series.

Rys. 5. Współczynnik oporu dyfuzyjnego dla poszczególnych serii.

Fig 6. Thermal conductivity coefficients of hemp-lime composite depending on the density of the material.

The author’s results are shown in black. Symbol descriptions are given in Table 3.

Rys. 6. Współczynniki przewodzenia ciepła kompozytu wapienno-konopnego w zależności od gęstości materiału. Wyniki autorów pokazano kolorem czarnym. Objaśnienie symboli z wykresu podano w Tabeli 3.

Fig. 7. The structure of hemp-lime composites with a hemp-lime ratio of 1:2 (right) and 1:1,5 (left).

Rys. 7. Struktury kompozytu wapienno-konopnego z proporcją paździerz do spoiwa 1:2 (po prawej) oraz 1:1,5 (po lewej).

Fig. 8. Summary of compressive strength results as determined at 10% deformation. Symbol descriptions are given in Table 3.

Rys. 8. Zestawienie wyników wytrzymałości na ściskanie określonej dla 10% odkształcenia. Objaśnienie symboli z wykresu podano w Tabeli 3.

Fig. 9. Comparison of diffusion resistance coefficient results. Symbol description are given in Table 3.

Rys. 9. Zestawienie wyników współczynnika oporu dyfuzyjnego. Objaśnienie symboli z wykresu podano w Tabeli 3.

Tab. 1. Binder compositions used in referenced studies.

Tab. 1. Składy spoiw zastosowane w badaniach.

Tab. 2. Proportions of ingredients for each series used in this study.

Tab. 2. Proporcje składników dla poszczególnych serii we własnych badaniach.

Tab. 3. Detailed summary of hemp-lime composite mix components and their properties. Results obtained from this study have a gray background.

Tab. 3. Szczegółowe zestawienie składów mieszanek kompozytów wapienno-konopnych i ich właściwości. Wyniki otrzymane w badaniach własnych wyszczególniono na szarym tle.

WPŁYW SKŁADU KOMPOZYTU WAPIENNO KONOPNEGO NA JEGO WŁAŚCIWOŚCI

MECHANICZNE I FIZYCZNE

Słowa kluczowe: hemcrete, kompozyt wapienno konopny, konopie przemysłowe, wytrzymałość na ściskanie, przewodność cieplna, współczynnik oporu dyfuzyjnego, zrównoważony materiał budowlany

STRESZCZENIE

W pracy przeanalizowano wpływ składu kompozytu wapienno konopnego na kluczowe właściwości mechaniczne i fizyczne. Artykuł zawiera wyniki badań wytrzymałości na ściskanie, paroprzepuszczalności oraz przewodności cieplnej kompozytu w zależności od składu mieszanek. Mieszanki różniły się między sobą składem spoiwa oraz proporcjami spoiwa do paździerz konopnych. Uzyskane wyniki porównano z wynikami z innej literatury naukowej. Na tej podstawie sformułowano wnioski, że skład spoiwa ma drugorzędne znaczenie na analizowane właściwości fizyczne i mechaniczne kompozytu wapienno konopnego.

W toku badań i analiz wyników wykazano, że kluczowy wpływ na właściwości kompozytu wapienno konopnego ma jego gęstość. Wykazano również, że zależy ona od proporcji spoiwa do kruszywa. Rodzaj zastosowanego spoiwa ma drugorzędne znaczenie dla właściwości materiału. Z tego powodu zaleca się stosować spoiwa jak najbardziej ekologiczne, takie jak metakaolin, aby wpływ materiału na środowisko był jak najniższy.

Analiza wyników, prowadzi do wniosku, że materiał powinien charakteryzować się gęstości wynoszącą około 380 kg/m³. Taką gęstość uzyskuje się dla proporcji spoiwa do paździerza wynoszącej 2. Przy większej ilości paździerza powstaje duża ilość makroporów, przez co przewodność cieplna nie zmniejsza się, natomiast wytrzymałość na ściskanie tak.

Wytrzymałość na ściskanie kompozytu wapienno konopnego po 28 dniach sezonowania nie zależy od składu spoiwa użytego w mieszance. Cecha ta związana jest przede wszystkim z proporcją spoiwa do paździerza. Dla zbadanych kompozytów wytrzymałość na ściskanie wynosiła od 0.32 do 0.57 MPa przy 20% odkształceniu. Materiał o takiej wytrzymałości na ściskanie nie jest rekomendowany by pełnić funkcję konstrukcyjną. Przy projektowaniu kompozytu wapienno konopnego kluczowym zadaniem jest uzyskanie wytrzymałości na ściskanie pozwalającej na pełnienie funkcji samonośnej przy możliwie niskim współczynniku przewodności cieplnej. Skład kompozytu wapienno konopnego nie ma większego wpływu na współczynnik oporu dyfuzyjnego, który w przeprowadzonych badaniach wyniósł zaledwie od 4-6. Wysoka paroprzepuszczalność może być zarówno zaletą jak i wadą m.in. ze względu na możliwość kondensacji pary wodnej w przegrodzie zewnętrznej. Dlatego też należy uwzględnić niską wartość oporu dyfuzyjnego przy projektowaniu przegród zewnętrznych budynków z kompozytu wapienno konopnego.

Dużą zaletą kompozytu wapienno konopnego jest jego ujemny ślad węglowy. Zwrócenie uwagi na koszt środowiskowy materiału przy planowaniu inwestycji wydaje się być kluczowy dla rozwoju kompozytu wapienno konopnego.

Received: 10.03.2020 Revised: 09.04.2020

